

UNCLASSIFIED

Defense Technical Information Center
Compilation Part Notice

ADP015785

TITLE: Photon Emission by Ions Interacting with Short Intense Laser Pulses

DISTRIBUTION: Approved for public release, distribution unlimited

This paper is part of the following report:

TITLE: The Proceedings of the International Laser Physics Workshop [LPHYS'01] [10th] Held in Moscow, Russia on July 3-7, 2001 [Laser Physics. Volume 12, Number 2]

To order the complete compilation report, use: ADA426515

The component part is provided here to allow users access to individually authored sections of proceedings, annals, symposia, etc. However, the component should be considered within the context of the overall compilation report and not as a stand-alone technical report.

The following component part numbers comprise the compilation report:
ADP015760 thru ADP015801

UNCLASSIFIED

Photon Emission by Ions Interacting with Short Intense Laser Pulses

N. J. Kylstra¹, R. M. Potvliege¹, and C. J. Joachain²

¹ Department of Physics, University of Durham, Durham, DH1 3LE, UK

² Physique Théorique, Université Libre de Bruxelles, CP227, Brussels, B-1050 Belgium

e-mail: R.M.Potvliege@durham.ac.uk

Received September 12, 2001

Abstract—Photon emission by a positive ion exposed to an intense few-cycle Ti:Sapphire laser pulse is studied within the strong field approximation. We find that the magnetic field component of the incident pulse has little effect below 10^{17} W cm⁻² peak intensity. However, for more intense pulses it significantly reduces photon emission and changes the plateau structure of the spectra, as compared to the predictions of the dipole approximation, and leads in certain parts of the spectrum to emission in the form of a single attosecond burst of X-ray photons. Results obtained by solving the time-dependent Schrödinger equation for a two dimensional model of atomic hydrogen interacting with an ultrashort high frequency laser pulse are also given for photon emission in the stabilization regime; for the case studied, the main effect of the pulse's magnetic field is to produce a relatively strong emission at the second harmonic frequency.

1. INTRODUCTION

Most theoretical studies of harmonic generation by atoms or ions have assumed that relativistic effects can be neglected and that the laser field can be described in the dipole approximation by a spatially homogeneous vector potential $A(t)$. The electric field component of the laser field is then given by $\mathcal{E}(t) = -dA(t)/dt$, and the magnetic field component vanishes, since $\mathcal{B}(t) = \nabla \times A(t) = 0$. However, this simple approach is inadequate for super-strong laser fields, as can be seen from the following argument. At high intensities, we can neglect the Coulomb interaction of the active electron with the core and, as a first approximation, treat its motion classically. Let us consider a laser pulse linearly polarized along \hat{x} and propagating along \hat{z} with wave vector $\mathbf{k} = k\hat{z}$, where $k = \omega/c$ and ω is the laser angular frequency. This pulse is described by the vector potential $A(\omega t - kz)\hat{x}$. To leading order in $1/c$, and employing atomic units (a.u.), the displacement of an electron initially at rest at the origin is given by

$$x(t) = \int_0^t A(\omega t') dt', \quad z(t) = \frac{1}{2c} \int_0^t A^2(\omega t') dt'. \quad (1)$$

The displacement in the propagation direction originates from the Lorentz force exerted by the magnetic field of the laser pulse on the oscillating electron, and increases monotonically during the pulse. In particular, for a step pulse of electric field amplitude \mathcal{E}_0 arriving at the origin at $t = 0$, we have

$$z(t) = \frac{\mathcal{E}_0^2}{2c\omega^2} \left[\frac{t}{2} + \frac{\sin(2\omega t)}{4\omega} \right]. \quad (2)$$

The drift per cycle in the propagation direction is $\chi_0 = \pi \mathcal{E}_0^2 / (2c\omega^3)$. It is found that for $\omega = 0.057$ a.u. (corresponding to a Ti:Sapphire laser of 800 nm wavelength) $\chi_0 \approx 1$ a.u. when the intensity is approximately 1×10^{15} W cm⁻², while for $\omega = 1$ a.u., $\chi_0 \approx 1$ a.u. when the intensity is approximately 5×10^{18} W cm⁻². Furthermore, the ejected electrons can be accelerated to relativistic velocities by the field if it is sufficiently intense. Relativistic effects should be expected to become important when the ponderomotive energy, U_p , approaches the rest energy of the electron, mc^2 . For a Ti: Sapphire laser of 800 nm wavelength, $U_p = mc^2$ at an intensity of 9×10^{18} W cm⁻². For a high-frequency laser field with angular frequency $\omega = 1$ a.u., this occurs at an intensity of 3×10^{21} W cm⁻². These intensities are much higher than those for which χ_0 is of the order of one Bohr radius. One can therefore distinguish three regimes of intensity, namely the "low intensity" regime, where the dipole approximation is applicable (except of course for inner shell transitions in heavy atoms), an intermediate regime where the magnetic drift is too large for the dipole approximation to be valid but the dynamics is still essentially non-relativistic, and the relativistic regime where the intensity is so high that relativistic effects must be taken into account.

In the present work, we investigate photon emission by atoms or positive ions irradiated by low frequency few-cycle laser pulses that are sufficiently intense that the magnetic field component of the pulse cannot be neglected. Research in this domain has been spurred by the development of laser systems capable of delivering ultra-short pulses consisting of only a few optical cycles, with peak intensities well above 10^{15} W cm⁻² [1]. Atoms or ions exposed to such pulses can experi-

ence much stronger laser fields before ionizing than would be possible in longer pulses, and this in turns permits the generation of photons of much higher energies. Moreover, positive ions can survive higher laser intensities than neutral atoms and therefore can generate more energetic photons [2–4]. In this paper, we focus on the case of photon emission by a multicharged ion driven by a Ti-Sapphire pulse in the intermediate regime of intensity where the magnetic drift is significant. We also briefly consider harmonic generation in the high frequency, strong-field stabilization regime.

2. PHOTON EMISSION IN A Ti:SAPPHIRE PULSE

High-order harmonic generation at low frequencies can be understood qualitatively in terms of a semi-classical recollision model [5–8]. This model, often called the “simple man’s model”, explains photon emission driven by intense low frequency laser fields as proceeding via several steps: In the first (bound–free) step, the active electron is detached from its parent ion (atom) core by tunneling ionization. In the second (free–free) step, the unbound electron interacts mainly with the laser field, so that its dynamics is essentially that of a free electron in the field, and can be treated to a good approximation using classical mechanics. As the phase of the field reverses, the electron can be accelerated back towards the parent core. Single ionization follows if the electron does not return to the core. However, if it does return, radiative recombination with the core may occur, in a third step, leading to harmonic generation.

A non-relativistic, fully quantum mechanical description of photon emission that incorporates the basic ideas of the simple man’s model has been developed within the dipole approximation by Lewenstein and co-workers [9, 10]. It has been extended to higher intensities, either by taking into account the magnetic drift of the electron within a non-dipole non-relativistic framework [11, 12] or by passing to a relativistic formulation based on the Klein–Gordon equation [13]. These theories make use of the strong field approximation (SFA), which consists of neglecting the interaction of the active electron with the core after it is detached by the field and before it scatters or recombines as it returns near the nucleus.

The present work follows the approach of [12]. Namely, we start from the nonrelativistic, non-dipole time-dependent Schrödinger equation (TADS) for a one-electron atom (ion) in a laser pulse linearly polarized along \hat{x} and propagating along \hat{z} . This equation reads, in a.u.,

$$i\frac{\partial}{\partial t}\Psi(\mathbf{r}, t) = \left\{ \frac{1}{2}[-i\nabla + \mathbf{A}(\eta)]^2 + V(r) \right\} \Psi(\mathbf{r}, t), \quad (3)$$

where $V(r)$ is the potential binding the electron and $\eta = \omega(t - z/c)$. To lowest order in $1/c$, we have $\mathbf{A}(\eta) = \mathbf{A}(\omega t) + (z/c)\mathcal{E}(\omega t)$. Transforming to the length gauge

by writing $\Psi^L(\mathbf{r}, t) = \exp[i\mathbf{A}(\omega t) \cdot \mathbf{r}]\Psi(\mathbf{r}, t)$, we obtain for $\Psi^L(\mathbf{r}, t)$ the non-dipole TDSE

$$i\frac{\partial}{\partial t}\Psi^L(\mathbf{r}, t) = \left\{ -\frac{1}{2}\nabla^2 + \left[\mathbf{r} - i\frac{z}{c}\nabla \right] \cdot \mathcal{E}(\omega t) + V(r) \right\} \Psi^L(\mathbf{r}, t). \quad (4)$$

An exact solution of equation (4) can be obtained when $V(r) = 0$. This non-relativistic, non-dipole Volkov wave function is given by [12]

$$\Phi_p(\mathbf{r}, t) = \frac{1}{(2\pi)^{3/2}} \exp \left(i\Pi(\mathbf{p}, t) \cdot \mathbf{r} - \frac{i}{2} \int [\Pi(\mathbf{p}, t'')]^2 dt'' \right), \quad (5)$$

with $\Pi(\mathbf{p}, t) = \mathbf{p} + \mathbf{A}(\omega t) + (1/c)[\mathbf{p} \cdot \mathbf{A}(\omega t) + A^2(\omega t)/2]\hat{z}$. Making the SFA and neglecting continuum-continuum transitions we approximate the dipole moment of the atom by the expression

$$\mathbf{d}(t) = \int_{-\infty}^{\infty} \langle \phi_0 | \mathbf{r} G_V^{(+)}(\mathbf{r}, t; \mathbf{r}', t') H_{\text{int}} | \phi_0 \rangle dt' + \text{c.c.}, \quad (6)$$

where $|\phi_0\rangle$ denotes the state vector of the field-free ground state of the atom (or ion), $H_{\text{int}} = [\mathbf{r}' - (ic)(\hat{x} \cdot \mathbf{r}')\nabla] \cdot \mathcal{E}(\omega t')$, and $G_V^{(+)}(\mathbf{r}, t; \mathbf{r}', t')$ is the non-dipole Volkov Green’s function,

$$G_V^{(+)}(\mathbf{r}, t; \mathbf{r}', t') = -i\theta(t - t') \int \Phi_p(\mathbf{r}, t) \Phi_p^*(\mathbf{r}', t') d\mathbf{p}. \quad (7)$$

The spectrum of the emitted photons is then obtained by calculating $|\hat{x} \cdot \mathbf{a}(\Omega)|^2$, for emission polarized parallel to the polarization direction of the incident pulse, and $|\hat{z} \cdot \mathbf{a}(\Omega)|^2$, for emission polarized along the direction of propagation of the incident pulse; in these expressions, Ω denotes the angular frequency of the emitted photon and $\mathbf{a}(\Omega)$ the Fourier transform of $\mathbf{d}(t)$. The ratio Ω/ω is an effective “harmonic order.” (Photons are emitted with a continuous distribution of frequencies, not at discrete harmonic frequencies, when the driving pulse is only a few optical cycles long.) Our results are obtained for a few-cycle pulse with carrier wavelength 800 nm and described by the vector potential

$$\mathbf{A}(\eta) = (\mathcal{E}_0/\omega) \sin^2(\eta/2N) \sin(\eta) \hat{x}, \quad (8)$$

where N is the number of optical cycles of the pulse.

The spectra presented in Fig. 1 are calculated for two-cycle pulses with peak intensities of 0.9, 1.8, and $3.6 \times 10^{17} \text{ W cm}^{-2}$, incident on a Li^{2+} or Be^{3+} ion. They supersede those reported in [12] for the same systems, which were affected by numerical inaccuracies. Results

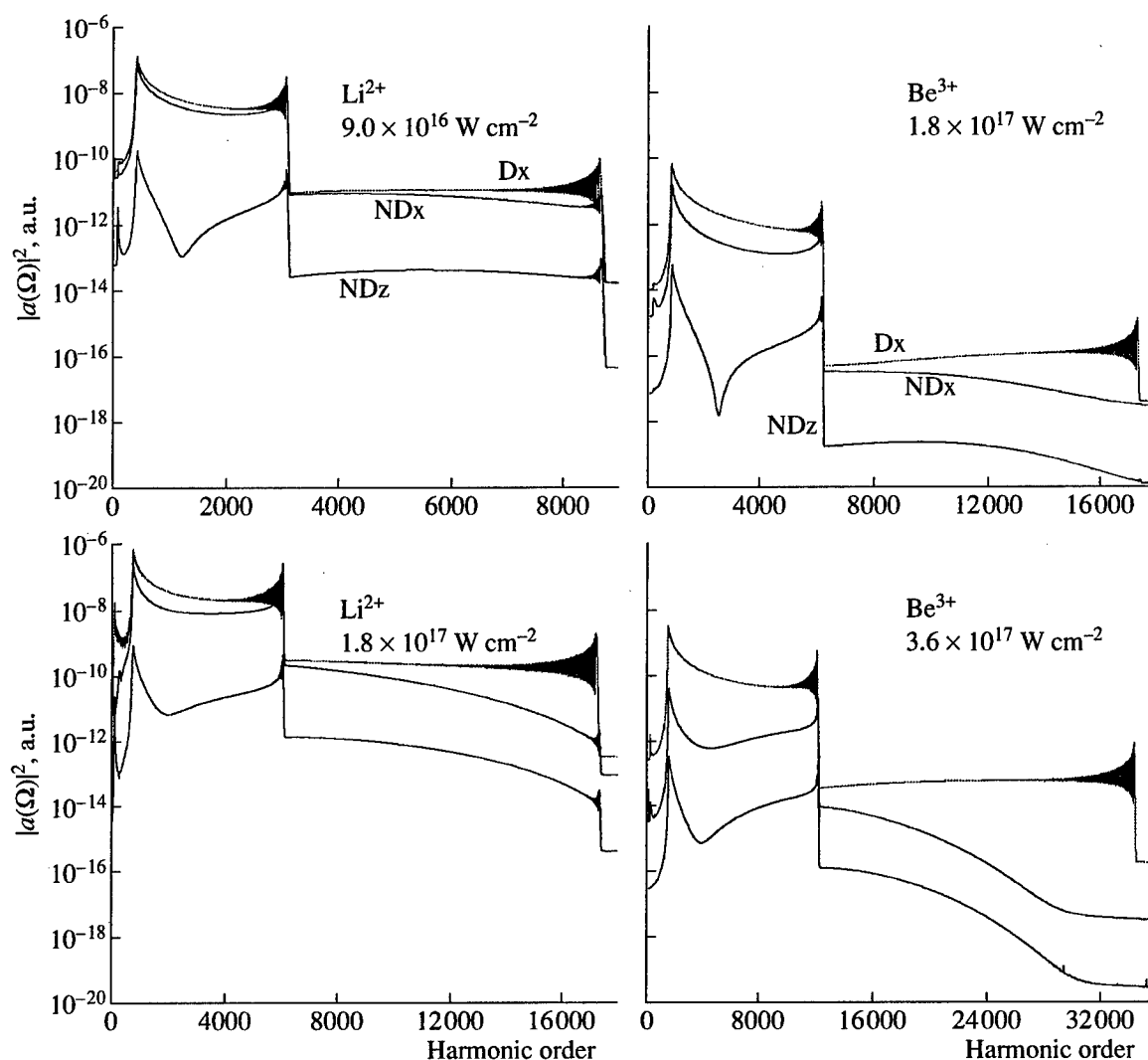


Fig. 1. The magnitude squared of the Fourier transform of the SFA dipole acceleration (in atomic units) of Li^{2+} (left) and Be^{3+} (right) as a function of the photon energy (in units of $\hbar\omega$). Dipole results (Dx) are displayed, as well as non-dipole results for photons polarized along \hat{x} (NDx) and \hat{z} (NDz). The incident laser pulse has a duration of two optical cycles, a carrier wavelength of 800 nm and the peak intensity indicated in each diagram.

obtained within the dipole approximation are also shown. The corresponding spectra for a four-cycle pulse with peak intensity $3.6 \times 10^{17} \text{ W cm}^{-2}$ are presented in Fig. 2. Apart for the deep minima in $|\hat{z} \cdot \mathbf{a}(\Omega)|^2$, which arise from destructive interferences, all the important features of the spectra of Figs. 1 and 2 can be understood within the simple man's model [4, 12]. For example, the two plateaus clearly visible in each diagram of Fig. 1 arise from the radiative recombination of electrons ionized within different half-cycle of the laser pulse. Each half-cycle contributes differently to the spectrum because of the rapid variation of the electric field amplitude during the pulse: more plateaus are visible in spectra of Fig. 2 since the pulse is longer. Emission polarized along the z -direction (i.e., the propagation direction of the incident field) is weaker than emission polarized along the x -direction; the difference is

typically two orders of magnitude at the highest intensity considered, and is larger in weaker fields. In this respect, it is worth noting that emission polarized in the z -direction is forbidden by the dipole selection rules and therefore would not occur if the magnetic field component of the pulse was neglected.

The influence of the magnetic field on photon emission polarized in the x -direction can be seen by comparing dipole and non-dipole results: above $10^{17} \text{ W cm}^{-2}$ peak intensity it significantly reduces the strength of photon emission, causes a "bending over" of the plateaus, and suppresses some of the cutoffs which separate the plateaus in the dipole spectra. The decrease in the strength of emission should be expected as the displacement in the z direction due to the magnetic drift, 317 a.u. per half cycle at $3.6 \times 10^{17} \text{ W cm}^{-2}$, is large enough to reduce considerably the overlap of the

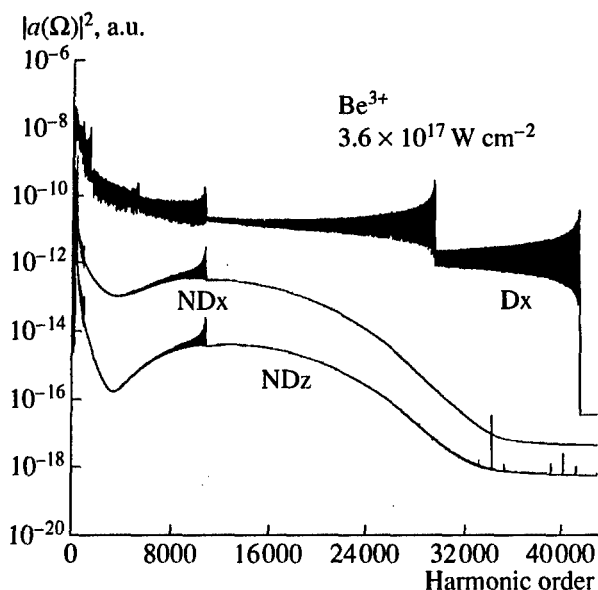


Fig. 2. The same as Fig. 1 but for Be^{3+} interacting with a four-cycle pulse.

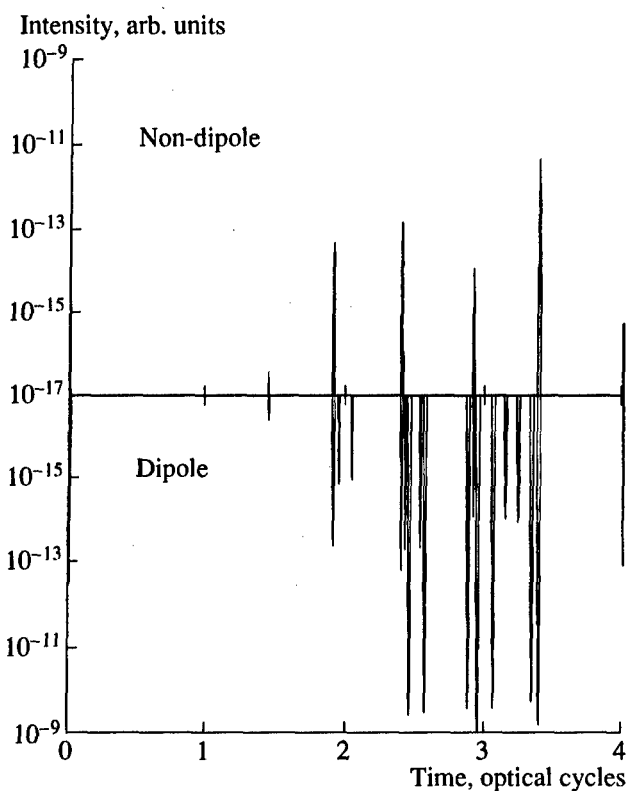


Fig. 3. The magnitude squared of the frequency-resolved dipole acceleration for emission of 3.9 keV photons by a single Be^{3+} ion interacting with a four-cycle Ti:Sapphire pulse of $3.6 \times 10^{17} \text{ W cm}^{-2}$ peak intensity. The results obtained within the dipole approximation are shown in the lower half of the diagram.

returning wave packet with the nucleus (if the electron is emitted in the direction of polarization of the field, as is assumed in the simple man's model) [14]. At $9.0 \times 10^{16} \text{ W cm}^{-2}$ the displacement is not sufficiently large compared to the width of the returning wave packet for having an important effect. Non-dipole effects in photon emission can be safely neglected below $10^{17} \text{ W cm}^{-2}$ peak intensity, at the Ti:Sapphire wavelength, but this is no longer the case for stronger fields [11, 12].

The bending over of the plateaus, which is also found in SFA calculations based on the Klein-Gordon equation [13], has the same origin as the overall decrease in the strength of photon emission. The magnetic drift incurred by the detached electrons before they recombine depend on their trajectory in the continuum. Since at any given time fast electrons are accelerated further along the positive z direction than slow electrons, the emission of high energy photons, which are produced by recombination of electrons that return to the nucleus with a high velocity, tends to be more suppressed than emission of low energy photons. The suppression may not always increase monotonically with energy, though, since emission at a given frequency is normally due to the recombination of electrons detached at different times during the pulse, following different trajectories, and thus deflected differently by the magnetic field. In fact, the trajectories that contribute most to photon emission in the dipole approximation and are responsible for the plateau structure of the spectra are often more deflected from the nucleus than trajectories that contribute little, leaving the non-dipole spectra to be dominated by the latter; hence the changes in the number and positions of the cutoff frequencies.

The influence of the magnetic field component of the laser pulse on the contribution to photon emission by different trajectories is illustrated in Fig. 3. The case considered is the same as in Fig. 2: photon emission by Be^{3+} interacting with a 4-cycle pulse of $3.6 \times 10^{17} \text{ W cm}^{-2}$ peak intensity. The quantity shown in this figure is the squared modulus of the frequency-resolved dipole acceleration, $a_{\Omega}(t)$, for emission polarized in the x -direction in a narrow frequency window centered about $\Omega = 2500\omega$. We define $a_{\Omega}(t)$ as [15]

$$a_{\Omega}(t) = \exp(-i\Omega t) \int \exp[-i(\omega - \Omega)t] \times F(\omega - \Omega) \hat{x} \cdot \mathbf{a}(\omega) d\omega, \quad (9)$$

where $F(\omega - \Omega)$ is a narrow Gaussian window centered at $\omega = \Omega$. For $\omega = 0.057 \text{ a.u.}$, photons with angular frequency $\Omega = 2500\omega$ have an energy of about 3.9 keV. The lower part of Fig. 3 shows $|a_{\Omega}(t)|^2$ calculated in the dipole approximation. Each spike in this diagram corresponds to a burst of emission of 3.9 keV photons. The spikes occur precisely at the instants where, in the simple man's model, detached electrons return at the nucleus with the speed required for emission at this energy. Seven bursts are particularly strong and have all

about the same intensity, showing that in the dipole approximation photon emission at $\Omega \approx 2500\omega$ is dominated by seven groups of trajectories. However, the magnetic drift, when taken into account, changes this picture dramatically. The upper part of the figure, where the non-dipole results are plotted, shows that all but one of the seven returns that contribute most in dipole approximation are suppressed to the point of not appearing in the graph anymore. The only one remaining occurs towards the end of the pulse and dominates the spectrum. The corresponding trajectory is less deflected than the others owing to the decrease in the strength of the magnetic field in the trailing edge of the pulse. As a consequence, emission in this region of the spectrum essentially consists of a single burst of X-ray photons. The width of the spike indicates that the duration of the burst is about 20 attoseconds. It is worth noting that the intensity of this photon emission depends crucially on how the envelope of the pulse decreases at the end of the pulse: the slower the decrease (e.g., the longer the pulse), the weaker the emission.

To summarize, we have seen that the force exerted on the electron by the magnetic field component of the pulse affects different parts of the spectra in different ways. It reduces photon emission above $1 \times 10^{17} \text{ W cm}^{-2}$ at the Ti:Sapphire wavelength, compared to the predictions of the dipole approximation; the reduction may depend sensitively on the temporal profile of the incident pulse. The magnetic drift also limits photon emission, in certain parts of the spectrum, to a single attosecond burst of X-rays.

3. PHOTON EMISSION IN A HIGH FREQUENCY PULSE

In the high frequency regime, atoms interacting with intense laser pulses can be relatively stable against ionization [16]. Recent investigations have demonstrated that, at sufficiently high intensities, the magnetic-field component of a short laser pulse can strongly influence the stabilization of atoms [17]. Atomic stabilization relies on the formation of a wavepacket that is localized at the turning points of a classical electron in the field. Therefore, beyond the dipole approximation, the magnetic-field induced drift in the propagation direction results in the wave packet moving away from the nucleus. This, in turn, leads to a breakdown of stabilization. This breakdown is expected to occur when the drift is of the order of 1 a.u. per optical cycle, which happens, as noted in the Introduction, at an intensity of about $5 \times 10^{18} \text{ W cm}^{-2}$ for an angular frequency of 1 a.u.

It is also of interest to investigate the influence of non-dipole effects on harmonic generation in the stabilization regime [18]. In Fig. 4 we show spectra obtained by integrating numerically the non-dipole time-dependent Schrödinger equation in two dimensions for the model hydrogen atom of [17]. The incident laser pulse is 4 cycles long, with the temporal profile defined by Eq. (8). Its angular frequency and peak intensity are

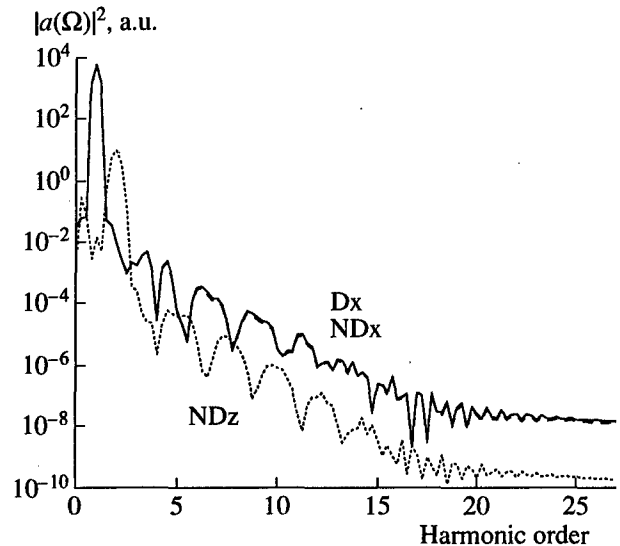


Fig. 4. The magnitude squared of the Fourier transform of the dipole acceleration (in atomic units) of a 2D model of atomic hydrogen, as a function of the photon energy (in units of $\hbar\omega$): (dashed curve) dipole results (Dx), (solid curve) non-dipole results for photons polarized along \hat{x} (NDx), (dotted curve) non-dipole results for photons polarized along \hat{z} (NDz). The incident laser pulse has a duration of four optical cycles and a peak intensity of $8 \times 10^{18} \text{ W cm}^{-2}$. The carrier angular frequency is $\omega = 1 \text{ a.u.}$

$\omega = 1 \text{ a.u.}$ and $8 \times 10^{18} \text{ W cm}^{-2}$. We obtain the dipole acceleration from the expectation value of the gradient of the potential and the expectation value of the momentum by applying Ehrenfest's theorem to the leading order in $1/c$:

$$\ddot{\mathbf{d}}(t) = -\langle \nabla V \rangle - \mathcal{E}(t) - [\langle \mathbf{p}(t) \rangle + \mathbf{A}(t)] \cdot \mathcal{E}(t)/c\hat{z}. \quad (10)$$

Photon emission polarized along the laser polarization direction is hardly affected by the magnetic-field induced drift, with dipole (Dx) and non-dipole (NDx) spectra being nearly indistinguishable in the frequency range spanned by the figure. Similar results have been obtained by Ryabikin and Sergeev [18] for a trapezoidal pulse of the same carrier wavelength and a peak intensity of $1.8 \times 10^{19} \text{ W cm}^{-2}$. In the case of Fig. 4, the non-dipole effects lead principally to a relatively strong emission at the second harmonic frequency, with the radiation polarized along the direction of propagation of the incident pulse. As can be seen from Eq. (2), this is the frequency at which a free classical electron driven by the field oscillates along the propagation direction.

REFERENCES

1. Brabec, T. and Krausz, F., 2000, *Rev. Mod. Phys.*, **72**, 545.
2. Preston, S.G., Sanpera, A., Zepf, M., Blyth, W.J., Smith, C.G., Wark, J.S., Key, M.H., Burnett, K., Nakai, N.,

- Neely, D., and Offenberger, A.A., 1996, *Phys. Rev. A*, **53**, R31.
3. Casu, M., Szymanowski, C., Hu, S., and Keitel, C.H., 2000, *J. Phys. B*, **33**, L411.
4. Potvliege, R.M., Kylstra, N.J., and Joachain, C.J., 2000, *J. Phys. B*, **33**, L743.
5. Kuchiev, M.Y., 1987, *JETP Lett.*, **45**, 404.
6. van Linden van den Heuvell, H.B. and Muller, H.G., 1988, Limiting Cases of Excess-Photon Ionization, *Multiphoton Processes*, Smith, S.J. and Knight, P.L., Eds. (Cambridge: Cambridge Univ. Press), p. 25.
7. Corkum, P.B., 1993, *Phys. Rev. Lett.*, **71**, 1994.
8. Kulander, K.C., Schafer, K.J., and Krause, J.L., 1993, Dynamics of Short-Pulse Excitation, Ionization and Harmonic Conversion, *Super-Intense Laser-Atom Physics*, Piraux, B., L'Huillier, A., and Rzazewski, K., Eds. (New York: Plenum), p. 95.
9. Lewenstein, M., Balcou, P., Ivanov, M.Y., L'Huillier, A., and Corkum, P., 1994, *Phys. Rev. A*, **49**, 2117.
10. Salières, P., L'Huillier, A., Antoine, P., and Lewenstein, M., 1999, *Adv. At. Mol. Opt. Phys.*, **41**, 83.
11. Walser, M.W., Keitel, C.H., Scrinzi, A., and Brabec, T., 2000, *Phys. Rev. Lett.*, **85**, 5082.
12. Kylstra, N.J., Potvliege, R.M., and Joachain, C.J., 2001, *J. Phys. B*, **34**, L55.
13. Milosević, D.B., Hu, X.S., and Keitel, C.H., 2001, *Phys. Rev. A*, **63**, 011403(R).
14. Kulyagin, R.V. and Taranukhin, V.D., 1997, *Laser Phys.*, **7**, 623.
15. Schafer, K.J. and Kulander, K.J., 1997, *Phys. Rev. Lett.*, **78**, 638.
16. Gavrilă, M., 2000, Stabilization of Atoms in Ultra-Strong Laser Fields: A Decade Later, *Multiphoton Processes*, DiMauro, L., Freeman, R.R., and Kulander, K.C., Eds. (AIP Conf. Proc.), no. 525, p. 103.
17. Vazquez de Aldana, J.R., Kylstra, N.J., Roso, L., Knight, P.L., Patel, A.S., and Worthington, R.A., 2001, *Phys. Rev. A*, **64**, 013411.
18. Ryabikin, M.Yu. and Sergeev, A.M., 2000, *Opt. Express*, **7**, 417.